

# BCl<sub>3</sub> Adsorption on Pristine, S-Doped, and Cr-Doped Graphynes: A DFT Study

Maryam Derakhshandeh (✉ [derakhshandehm2020@gmail.com](mailto:derakhshandehm2020@gmail.com))  
Islamic Azad University

---

## Research Article

**Keywords:** Sensor, Density functional theory, BCl<sub>3</sub>, graphyne, adsorption, Nanosheet

**Posted Date:** May 13th, 2021

**DOI:** <https://doi.org/10.21203/rs.3.rs-512555/v1>

**License:**  This work is licensed under a Creative Commons Attribution 4.0 International License.

[Read Full License](#)

---

**BCl<sub>3</sub> adsorption on pristine, S-doped, and Cr-doped graphynes: a DFT Study**

**Maryam Derakhshandeh**

Department of chemistry, faculty of chemical engineering, Mahshahr branch, Islamic Azad  
university, Mahshahr, Iran

**Email:** [derakhshandehm2020@gmail.com](mailto:derakhshandehm2020@gmail.com)

## **Abstract**

The adsorption of boron trichloride ( $\text{BCl}_3$ ) was explored onto pristine, S-doped, and Cr-doped graphyne through density functional theory computations. The interaction of  $\text{BCl}_3$  with pristine graphyne was weak and, thus, this sheet cannot be used as a sensor. Although S-doping strengthens the interaction, the S-doped sheet cannot still be used as a sensor. However, the reactivity and sensitivity of the sheet are significantly increased toward  $\text{BCl}_3$  by replacing the C atom of graphyne with the transition metal Cr. The HOMO-LUMO gap of Cr-doped graphyne reduces from 2.18 to 1.38 eV following the adsorption of  $\text{BCl}_3$ , which significantly increases the electrical conductivity. Thus, the great change in the conductivity can be converted into an electronic signal, indicating that Cr-doped graphyne may be a promising sensor for  $\text{BCl}_3$ . Also, its work function is considerably decreased by the adsorption process, indicating that it can also work as a work function-type sensor for  $\text{BCl}_3$  detection.

**Keywords:** Sensor, Density functional theory,  $\text{BCl}_3$ , graphyne, adsorption, Nanosheet

## 1. Introduction

Bromine trichloride ( $\text{BCl}_3$ ) is a dangerous toxic substance that can be used to refine copper, zinc, magnesium, and aluminum alloys to remove carbides, nitrides, and oxides from molten metal. It is used as a source of boron to increase the amount of British thermal unit for use in the propulsion of rockets and high-energy fuels [1]. Therefore, it is very important to identify this dangerous gas, which has rarely been addressed. The large surface area of nanostructures is highly susceptible to the adsorption of gas molecules, for example, the graphene nanoplate has been used as a sensor to adsorb many hazardous gases [2, 3]. In addition, the electronic properties of this nanostructure are sensitive toward the presence of chemical vapors, which is the reason for the attraction of these materials to nanostructures [4-6]. Also, doping is a method that is used to enhance the sensitivity of electronic properties and the adsorption performance of nanostructures [7].

Graphyne nanosheet is one of the carbon allotropes proposed in 1987 by Baughman et al [8]. It is composed of a crystal lattice consisting of carbon with  $sp$  and  $sp^2$  hybridization. Carbon, which participates in the formation of a hexagonal ring by  $sp^2$  hybridization, and another carbon, by  $sp$  hybridization which binds these hexagonal rings together. The difference between this nanosheet and graphene is the many triple bonds it has in its network structure, which greatly changes its electronic and optical properties [9]. The advantages of this change are high chemical stability, large surface area and high electrical conductivity of graphyne [10-12]. A wide range of applications has been defined for graphyne, for example in electronics, chemical sensors, energy storage systems, and as electrodes in batteries [13-16]. The aim of the present work is to investigate the adsorption of  $\text{BCl}_3$  onto graphyne nanosheets to find an easy and fast way to identify this gas using density functional theory calculations.

## 2. Computational methods

An 86-carbon graphyne nanosheet was selected as an adsorbent for  $\text{BCl}_3$ . Hydrogen atoms were used to saturate its ends to decrease the boundary effects. All calculations such as energy calculations, geometry optimization, and state density analysis on pristine, Cr-doped and S-doped graphyne were carried out through augmented B3LYP, i.e, B3LYP-D\*. Here, Grimme's "D" term for evaluating dispersion forces that are weak. As a basis set, 6-31G (d) was used and all calculations were done by using GAMESS software [11]. We used GaussSum [17] software to draw the density of state (DOS) diagram. Based on previous studies, B3LYP is used for nanostructures and it exhibits high performance in the field [18-20].

After the adsorption of the  $\text{BCl}_3$  molecule onto pure graphyne as well as S-doped and Cr-doped graphyne, its adsorption energy is calculated by the equation below:

$$E_{ad} = E(\text{BCl}_3) + E(\text{sheet}) - E(\text{BCl}_3/\text{sheet}) - E_{BSSE} \quad (1)$$

Here,  $E(\text{sheet})$  is pure or doped graphyne sheet energy,  $E(\text{BCl}_3)$  is the  $\text{BCl}_3$  molecule energy,  $E(\text{BCl}_3/\text{sheet})$  designates the energy of the sheet that adsorbed the  $\text{BCl}_3$  molecule. For the structures under study, the positive energy of the adsorption shows that this adsorption is exothermic. The correction of the basis set superposition error was making for interactions. The HOMO-LUMO energy gap ( $E_g$ ) was computed according to the following equation:

$$E_g = E_{LUMO} - E_{HOMO} \quad (2)$$

Where  $E_{LUMO}$  and  $E_{HOMO}$  designate the energy of the lowest and the highest unoccupied molecular orbitals respectively.

### 3. Results and discussion

#### 3.1. Pristine graphyne

Graphyne is one of the carbon allotropes in which single, resonance bonds (in its hexagonal ring) and triple bonds ( $-C\equiv C-$ ) between its carbons can be seen, as shown Figure 1. As mentioned earlier, it has two types of carbon atoms in terms of hybridization, one is  $sp$ -hybridized (tagged as C1), which connects carbon hexagons, and the other is  $sp^2$ -hybridized hexagons (tagged as C2). After the optimization procedure was performed, the bond length between the carbons in the hexagonal ring was computed to be  $1.42\text{\AA}$ , which indicates the existence of a resonant bond between them. There is a bond length of  $1.22\text{\AA}$  between the two carbon atoms of C2, which suggests a triple bond. Furthermore, the bond length C1-C2 bond length is  $1.41\text{\AA}$ . By comparing it with the bond between two carbons of ethane ( $\sim 1.53\text{\AA}$ ), it can be inferred that there is a resonance  $\pi$  bond between the two C1 and C2 carbons. Due to the presence of C2 atoms in graphyne, this configuration is more unstable in terms of energy than graphene [7]. To obtain the most stable  $BCl_3$  that is adsorbed onto graphyne configuration, we evaluated various interaction models. We showed at least three states by considering the  $BCl_3$  molecule parallel to the sheet and in two states perpendicular to the graphyne sheet, and compared them to find the most stable state (Fig. 2). The data obtained from the optimization of these configurations are given in Table 1.

The results of Fig. 2 show that complex **A** is the most stable complex for this type of interaction. However, with  $E_{ad}$  of  $13.21\text{ kcal/mol}$ , it exhibits a van der Waals interaction which is weak. The interaction of **B** and **C** complexes with adsorption energies of  $10.87$  and  $10.21\text{ kcal/mol}$ , respectively, are weaker than those of complex **A**. The most stable  $BCl_3$ /graphyne (**A**) configuration was obtained, in which the  $BCl_3$  molecule interacted with the graphyne sheet horizontally with an equilibrium distance of  $3.23\text{\AA}$  and an  $E_{ad}$  of  $13.21\text{ kcal/mol}$ , and these observations confirm that the interaction is weak. According to Table 1 and as shown in Fig. 1, the graphyne  $E_g$  is  $2.57\text{eV}$ , which is reduced to  $2.26$ ,  $2.42$ , and  $2.51\text{eV}$  for configurations **A**, **B**, and **C**,

respectively, which is not a significant change. Therefore, graphyne is still a semiconductor after the adsorption of  $\text{BCl}_3$  because the weak adsorption of  $\text{BCl}_3$  occurs without a large change in  $E_g$ .

### 3.2. S-doped graphyne

After replacing one of the C1 and C2 atoms in graphyne, the optimized structures are shown in Fig. 3. It is understood that after the sulfide (S) atom is doped in the graphyne nanosheet, the geometric structures of these nanosheets are distorted. Also, since the S atom is larger than the carbon atom, it is placed outside of the graphyne nanosheet structure. Here, we show S-doped as **S.1** and **S.2**, that C1 atom C2 atom are replaced by S, respectively. Based on the calculations of the bond lengths, the S-C bonds are longer than the carbon-carbon bonds in the pristine sheet. The lengths of S-C1 and S-C2 bonds are 1.84 and 1.63 Å, respectively.  $E_g$  of these configurations have not changed much compared to the pristine graphyne, reaching 2.51 eV in complex **S.1** and 2.45 eV in complex **S.2**, indicating that these configurations are semiconductors. At this stage, we placed the  $\text{BCl}_3$  molecule on top of the S with different orientations to study the interaction of these doped nanosheets with this molecule. After optimizing these structures, the  $\text{BCl}_3$  molecule was placed onto the S-doped graphyne surface in a parallel fashion, as shown in Fig. 4. The amount of  $E_{\text{ad}}$  was obtained to be 15.62 kcal/mol for complex **E**, and 15.75 kcal/mol for complex **F**, indicating that the interaction is almost weak.

### 3.2. Cr-doped graphyne

Moreover, in the graphyne sheet, instead of C1 and C2 atoms, a chromium (Cr) atom is replaced and its influence is explored over the geometric structure and electronic characteristics of the graphyne sheet (Fig. 5). The Cr atom in the graphyne nanosheet disrupts its geometric structure because it is larger than carbon, and it was placed slightly higher than the surface of the sheet (Fig. 5). The Cr-C bonds are longer than the carbon-carbon bonds in the graphyne sheet, Cr-C1 and Cr-

C2 bond lengths are 1.88 and 1.67 Å, respectively. The Cr-doped graphyne data are provided in Table 3. The  $E_g$  for structure **Cr.1** is 2.30 eV and it is 2.18 eV for **Cr.2**, which is decreased compared to  $E_g$  of the pristine graphyne sheet. However, the Cr-doped graphyne nanosheets are still semiconductors.

To investigate the interaction between the  $\text{BCl}_3$  molecule and Cr-doped graphyne, the  $\text{BCl}_3$  molecule was placed in different directions above the Cr atom (shown in Fig. 6). Two of the orientations were shown to be local minima, which we introduced as **N** and **M**. In these configurations, the  $\text{BCl}_3$  molecule is located at the top of the Cr atom and the bond length is 2.56 and 2.89 Å, respectively, and  $E_{\text{ad}}$  was obtained. For configuration **M**,  $E_{\text{ad}}$  is 26.56 kcal/mol and it is 47.02 kcal/mol for configuration **N**. The results indicate that Cr-doping significantly increases the reactivity of graphyne toward the  $\text{BCl}_3$  molecule compared to S-doping. This is due to the fact that the lone pairs on the S atom repel the lone pairs of the Cl atoms of  $\text{BCl}_3$  and prevent the interaction. Also, it cannot directly interact with the electron deficient B atom of  $\text{BCl}_3$  because of a steric effect.

According to Table 3, Cr-doping is capable of increasing the graphyne nanosheet sensitivity toward the  $\text{BCl}_3$  molecule. The partial DOS plot shows that a new occupied orbital appears on the Cr-doped graphyne nanosheet at -4.08 eV due to the presence of  $\text{BCl}_3$ . The HOMO profile shown in Fig. 8 also confirms that the HOMO of complex shifts on the  $\text{BCl}_3$  with changing the HOMO energy. The  $E_g$  of Cr-doped graphyne decreases significantly following the adsorption of  $\text{BCl}_3$  and the sheet becomes more conductive. Numerically, its  $E_g$  in complex **M** decreased from 2.30 to 1.92 eV (by approximately 16.5%) and in complex **N** from 2.18 to 1.37 eV (~ 37.1%). The electrical conductivity of the sheet which was doped with Cr can change because of this change based on the equation below:

$$\sigma \propto \exp\left(\frac{-E_g}{2kT}\right) \quad (3)$$

In this equation,  $k$  designates the Boltzmann constant and  $\sigma$  is the electrical conductivity [21]. At a constant temperature, the lower the amount of  $E_g$ , the higher the electrical conductivity. So, when the adsorption procedure causes a decrease in  $E_g$ , the electrical conductance of Cr-doped graphyne increases significantly. To better evaluate the sensitivity of the configurations under study, the changes in the work function ( $\Phi$ ) were investigated before and following the adsorption process.  $\Phi$  of a semiconductor is the least amount of work needed for extracting an electron from the Fermi level. The re-examination of the gas-induced  $\Phi$  by the suspended amplitude effect modifiers has been accepted for several years as the basis for the realization of a sensor operating system [22].

Theoretically, in vacuum, the released electron current densities are defined as follows:

$$j = AT^2 \exp\left(\frac{-\Phi}{kT}\right) \quad (4)$$

Where  $A$  designates the Richardson constant ( $A/m^2$ ),  $T$  designates the temperature (K).  $\Phi$  designates the work function as mentioned above. We computed the  $\Phi$  values as follows:

$$\Phi = E_{\text{inf}} - E_F \quad (5)$$

Where  $E_F$  designates the energy of the Fermi level and  $E_{\text{inf}}$  designates the electrostatic potential at infinity, which is presumed to be equal to 0. We subtracted  $\Phi$  of the sheet from that of the complexes and obtained  $\Phi$  changes ( $\Delta\Phi$ ).  $\Phi$  for pristine graphyne was about 3.90 eV and changed very slightly after adsorbing the  $\text{BCl}_3$  molecule, which can be ignored. Also, changes in  $\Phi$  of S-doped graphyne are very small after  $\text{BCl}_3$  is adsorbed. But when  $\text{BCl}_3$  is adsorbed onto Cr-doped graphyne,  $\Phi$  is significantly reduced from 3.81 to 3.39 eV. According to Eq. 4, there is an exponential relationship between the emitted current density and  $\Phi$ . Therefore, it can be said that

after the adsorption of  $\text{BCl}_3$ , by decreasing the  $\Phi$ , the current density of the emitted electron increases dramatically. Accordingly, we think that Cr-doping in graphyne is a promising way to increase the sensitivity of graphyne toward  $\text{BCl}_3$  which pristine graphyne did not.

#### **4. Conclusions**

The interaction of  $\text{BCl}_3$  was explored with pristine, S-doped, and Cr-doped graphyne by using density functional theory calculations. In the most stable  $\text{BCl}_3$ /graphyne nanosheet complex,  $\text{BCl}_3$  is adsorbed onto the surface of the nanosheet in a parallel fashion with  $E_{\text{ad}}$  of 13.21 kcal/mol. It is found that the adsorption of the  $\text{BCl}_3$  molecule onto pure and S-doped graphyne is weak with low  $E_{\text{ad}}$ . Adsorption of the  $\text{BCl}_3$  molecule could not change the electronic properties of pure, and S-doped graphyne nanosheets significantly. But the  $\text{BCl}_3$  molecule showed strong interactions with the Cr-doped graphyne nanosheets with  $E_{\text{ad}}$  of 47.02 kcal/mol. The  $\text{BCl}_3$  adsorption changes the electrical conductivity of Cr-doped graphyne to a great extent. Therefore, we think that Cr-doped graphyne could be a promising sensor for detecting  $\text{BCl}_3$ . Also, after the  $\text{BCl}_3$  adsorption, by decreasing  $\Phi$ , the current density of the emitted electron increases dramatically. This shows that Cr-doped graphene may be a  $\Phi$ -type sensor for  $\text{BCl}_3$ .

## References

- [1] M. Lin, Z. Fan, Z. Ma, L. Allen, H. Morkoc, Reactive ion etching of GaN using BCl<sub>3</sub>, *Applied Physics Letters*, 64 (1994) 887-888.
- [2] G.K. Walia, D.K.K. Randhawa, Adsorption and dissociation of sulfur-based toxic gas molecules on silicene nanoribbons: a quest for high-performance gas sensors and catalysts, *Journal of molecular modeling*, 24 (2018) 1-8.
- [3] C. Tabtimsai, W. Rakrai, S. Phalinyot, B. Wannoo, Interaction investigation of single and multiple carbon monoxide molecules with Fe-, Ru-, and Os-doped single-walled carbon nanotubes by DFT study: applications to gas adsorption and detection nanomaterials, *Journal of Molecular Modeling*, 26 (2020) 1-13.
- [4] M. Xiao, P. Liu, Adsorption of acetylsalicylic acid on the aluminum nitride nanotube in both gas and solvent medium: a DFT study, *Journal of Molecular Modeling*, 26 (2020) 1-8.
- [5] B. Sütay, M. Yurtsever, Adsorption of dihalogen molecules on pristine graphene surface: Monte Carlo and molecular dynamics simulation studies, *Journal of molecular modeling*, 23 (2017) 150.
- [6] J. Kaur, R. Kumar, R. Vohra, R.S. Sawhney, A pursuit to design highly sensitive fullerene-based sensors: adsorption and dissociation phenomenon of toxic sulfur gases on B 40 fullerene, *Journal of molecular modeling*, 26 (2020) 1-13.
- [7] A.A. Peyghan, S.F. Rastegar, N.L. Hadipour, DFT study of NH<sub>3</sub> adsorption on pristine, Ni- and Si-doped graphynes, *Physics Letters A*, 378 (2014) 2184-2190.
- [8] R. Baughman, H. Eckhardt, M. Kertesz, Structure-property predictions for new planar forms of carbon: Layered phases containing sp<sup>2</sup> and sp atoms, *The Journal of chemical physics*, 87 (1987) 6687-6699.

- [9] B. Bhattacharya, N. Singh, R. Mondal, U. Sarkar, Electronic and optical properties of pristine and boron–nitrogen doped graphyne nanotubes, *Physical Chemistry Chemical Physics*, 17 (2015) 19325-19341.
- [10] J. Kang, J. Li, F. Wu, S.-S. Li, J.-B. Xia, Elastic, electronic, and optical properties of two-dimensional graphyne sheet, *The Journal of Physical Chemistry C*, 115 (2011) 20466-20470.
- [11] S.W. Cranford, M.J. Buehler, Mechanical properties of graphyne, *Carbon*, 49 (2011) 4111-4121.
- [12] Y. Zhang, Q. Pei, C. Wang, Mechanical properties of graphynes under tension: a molecular dynamics study, *Applied Physics Letters*, 101 (2012) 081909.
- [13] J. Beheshtian, M.T. Baei, A.A. Peyghan, Z. Bagheri, Electronic sensor for sulfide dioxide based on AlN nanotubes: a computational study, *Journal of molecular modeling*, 18 (2012) 4745-4750.
- [14] S. Saha, T.C. Dinadayalane, J.S. Murray, D. Leszczynska, J. Leszczynski, Surface reactivity for chlorination on chlorinated (5, 5) armchair SWCNT: a computational approach, *The Journal of Physical Chemistry C*, 116 (2012) 22399-22410.
- [15] J. Beheshtian, A.A. Peyghan, Z. Bagheri, Adsorption and dissociation of Cl<sub>2</sub> molecule on ZnO nanocluster, *Applied surface science*, 258 (2012) 8171-8176.
- [16] J. Deb, B. Bhattacharya, N.B. Singh, U. Sarkar, First principle study of adsorption of boron-halogenated system on pristine graphyne, *Structural Chemistry*, 27 (2016) 1221-1227.
- [17] N.M. O'boyle, A.L. Tenderholt, K.M. Langner, CcLib: a library for package-independent computational chemistry algorithms, *Journal of computational chemistry*, 29 (2008) 839-845.
- [18] M.T. Baei, A.A. Peyghan, Z. Bagheri, M.B. Tabar, B-doping makes the carbon nanocones sensitive towards NO molecules, *Physics Letters A*, 377 (2012) 107-111.

- [19] K. Adhikari, A. Ray, Carbon-and silicon-capped silicon carbide nanotubes: an ab initio study, *Physics Letters A*, 375 (2011) 1817-1823.
- [20] G. Zhao, X. Li, M. Huang, Z. Zhen, Y. Zhong, Q. Chen, X. Zhao, Y. He, R. Hu, T. Yang, The physics and chemistry of graphene-on-surfaces, *Chemical Society Reviews*, 46 (2017) 4417-4449.
- [21] S.S. Li, *Semiconductor physical electronics*, Springer Science & Business Media, 2012.
- [22] S. Stegmeier, M. Fleischer, P. Hauptmann, Influence of the morphology of platinum combined with  $\beta$ -Ga<sub>2</sub>O<sub>3</sub> on the VOC response of work function type sensors, *Sensors and Actuators B: Chemical*, 148 (2010) 439-449.

## Figure captions

**Fig. 1.** Optimized structure of graphyne and its density of state (DOS).

**Fig. 2.** Models for three stable adsorption states for a  $\text{BCl}_3$  molecule on the pristine graphyne, distances are in Å.

**Fig. 3.** Optimized structures of different S-doped graphyne.

**Fig. 4.** Models for two stable adsorption states for a  $\text{BCl}_3$  molecule on the different S-doped graphyne, distances are in Å.

**Fig. 5.** Optimized structures of different Cr-doped graphyne.

**Fig. 6.** Models for two stable adsorption states for a  $\text{BCl}_3$  molecule on the different Cr-doped graphyne, distances are in Å.

**Fig. 7.** Partial DOS plot of Cr-doped graphyne/  $\text{BCl}_3$  nanostructure complex.

**Fig. 8.** The HOMO profile of Cr-doped graphyne/  $\text{BCl}_3$  nanostructure complex.

**Table 1.** Calculated adsorption energy ( $E_{\text{ad}}$ , kcal/mol), HOMO energies ( $E_{\text{HOMO}}$ ), LUMO energies ( $E_{\text{LUMO}}$ ), Fermi level energies ( $E_{\text{F}}$ ), HOMO–LUMO energy gap ( $E_{\text{g}}$ ) and work function ( $\Phi$ ) for pristine graphyne.

Structure	$E_{\text{ad}}$	$E_{\text{HOMO}}$	$E_{\text{F}}$	$E_{\text{LUMO}}$	$E_{\text{g}}$	$\Delta E_{\text{g}}(\%)$	$\Phi$	$\% \Delta \Phi$
Graphyne	-	-5.18	-3.90	-2.62	2.56	-	3.90	-
<b>A</b>	13.21	-5.01	-3.88	-2.75	2.26	-11.7	3.88	-0.5
<b>B</b>	10.87	-5.10	-3.89	-2.68	2.42	-5.5	3.89	-0.2
<b>C</b>	10.21	-5.15	-3.89	-2.64	2.51	-1.9	3.89	-0.2

**Table 2.** Calculated adsorption energy ( $E_{ad}$ , kcal/mol), HOMO energies ( $E_{HOMO}$ ), LUMO energies ( $E_{LUMO}$ ), Fermi level energies ( $E_F$ ), HOMO–LUMO energy gap ( $E_g$ ) and work function ( $\Phi$ ) for S-doped graphyne.

Structure	$E_{ad}$	$E_{HOMO}$	$E_F$	$E_{LUMO}$	$E_g$	$\Delta E_g(\%)$	$\Phi$	$\% \Delta \Phi$
<b>S.1</b>	-	-5.16	-3.90	-2.65	2.51	-	3.90	-
<b>E</b>	15.62	-5.00	-3.83	-2.66	2.34	-6.7	3.83	-1.8
<b>S.2</b>	-	-5.12	-3.89	-2.67	2.45	-	3.89	-
<b>F</b>	15.75	-4.92	-3.81	-2.70	2.22	-9.4	3.81	-2.1

**Table 3.** Calculated adsorption energy ( $E_{ad}$ , kcal/mol), HOMO energies ( $E_{HOMO}$ ), LUMO energies ( $E_{LUMO}$ ), Fermi level energies ( $E_F$ ), HOMO–LUMO energy gap ( $E_g$ ) and work function ( $\Phi$ ) for Cr-doped graphyne.

Structure	$E_{ad}$	$E_{HOMO}$	$E_F$	$E_{LUMO}$	$E_g$	$\Delta E_g(\%)$	$\Phi$	$\% \Delta \Phi$
<b>Cr.1</b>	-	-4.98	-3.83	-2.68	2.30	-	3.83	-
<b>M</b>	26.56	-4.70	-3.74	-2.78	1.92	-16.5	3.74	-2.3
<b>Cr.2</b>	-	-4.90	-3.81	-2.72	2.18	-	3.81	-
<b>N</b>	47.02	-4.12	-3.43	-2.75	1.37	-37.1	3.43	-9.8

Fig. 1.

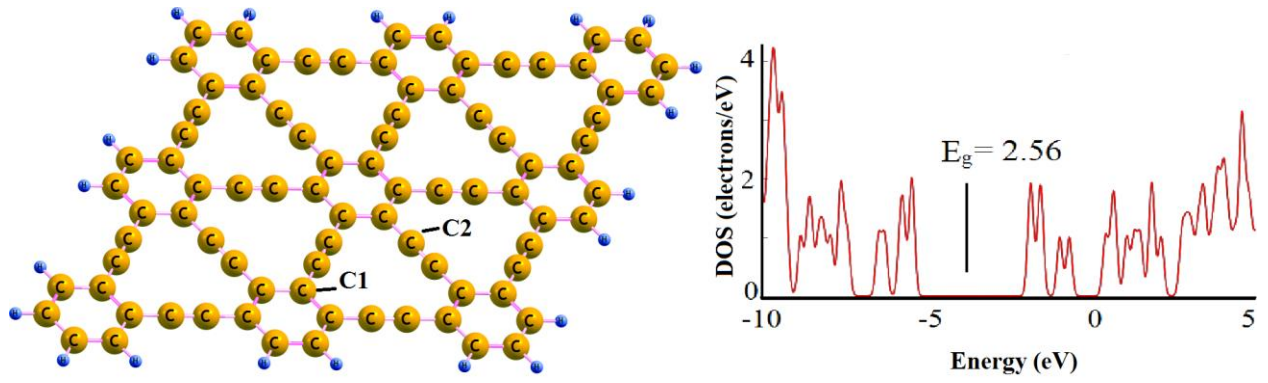


Fig. 2.

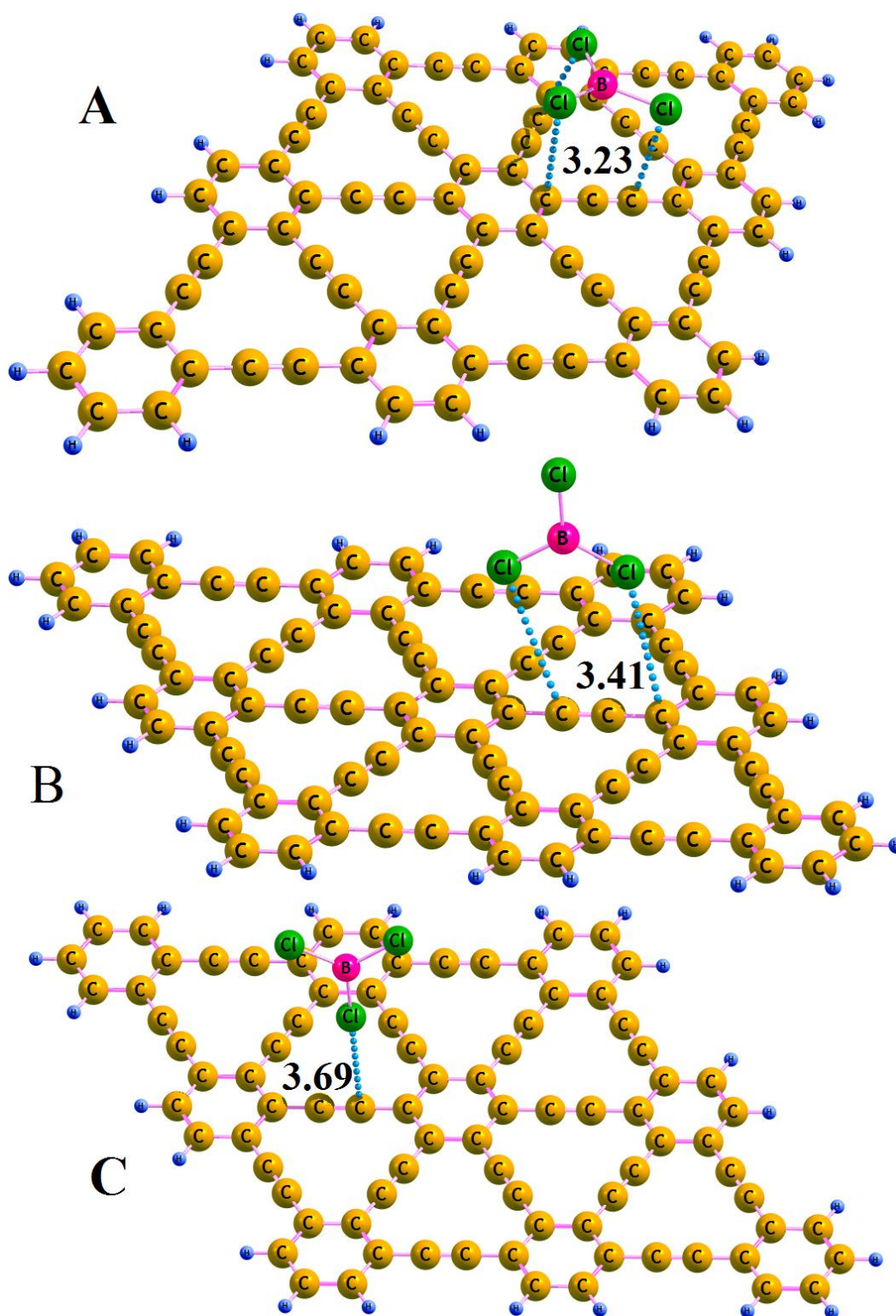


Fig. 3.

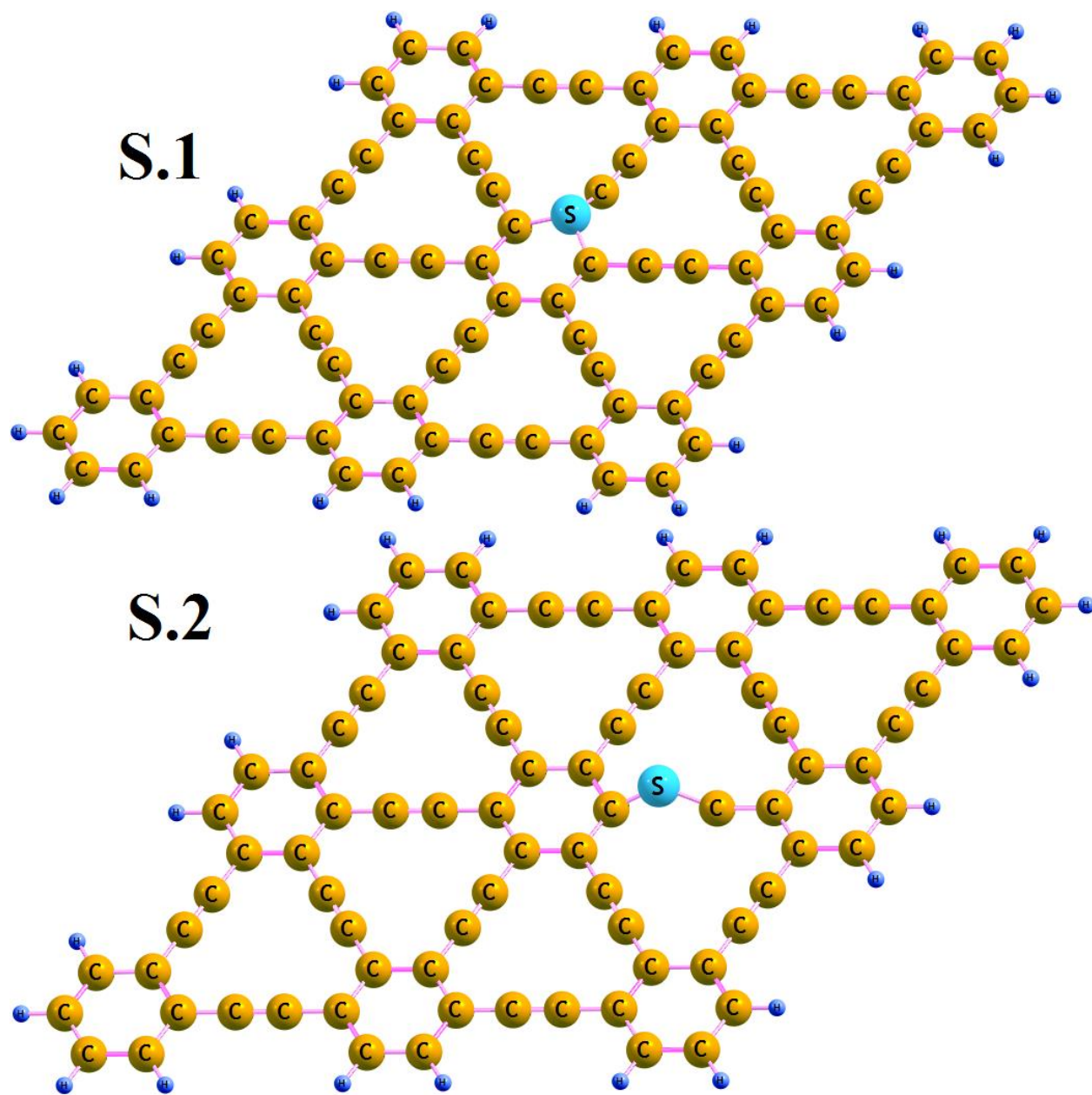


Fig. 4.

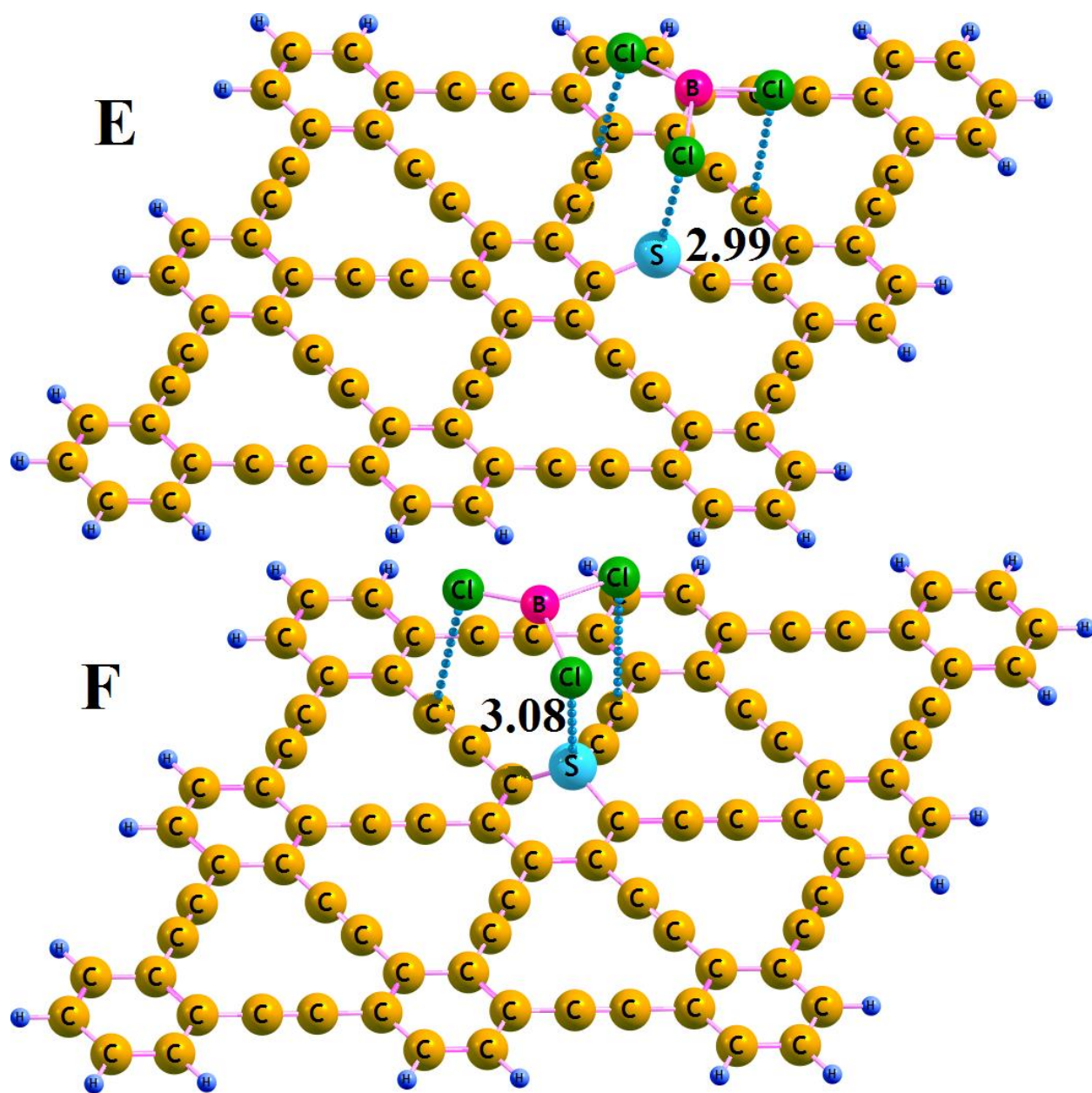


Fig. 5.

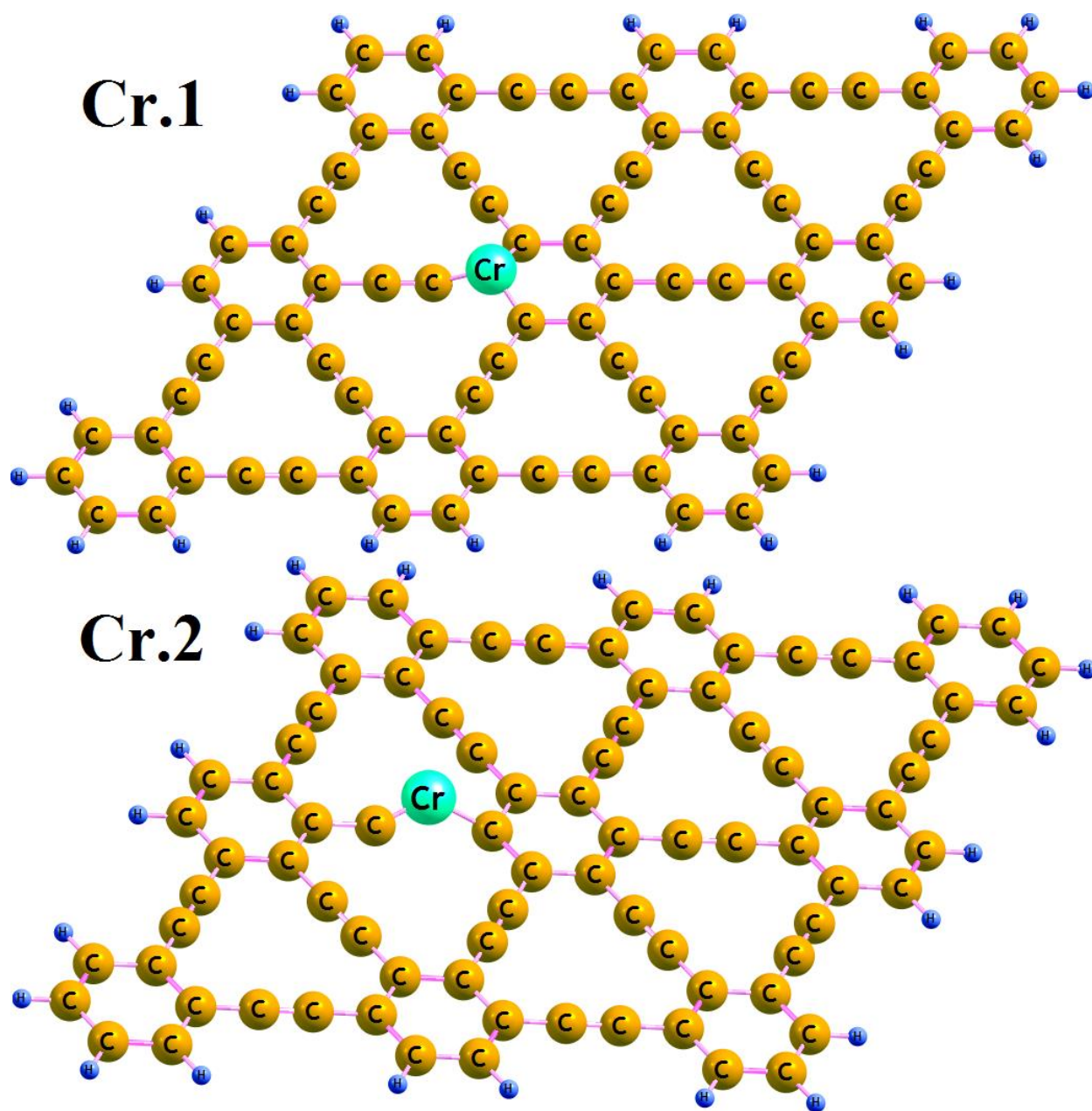


Fig. 6.

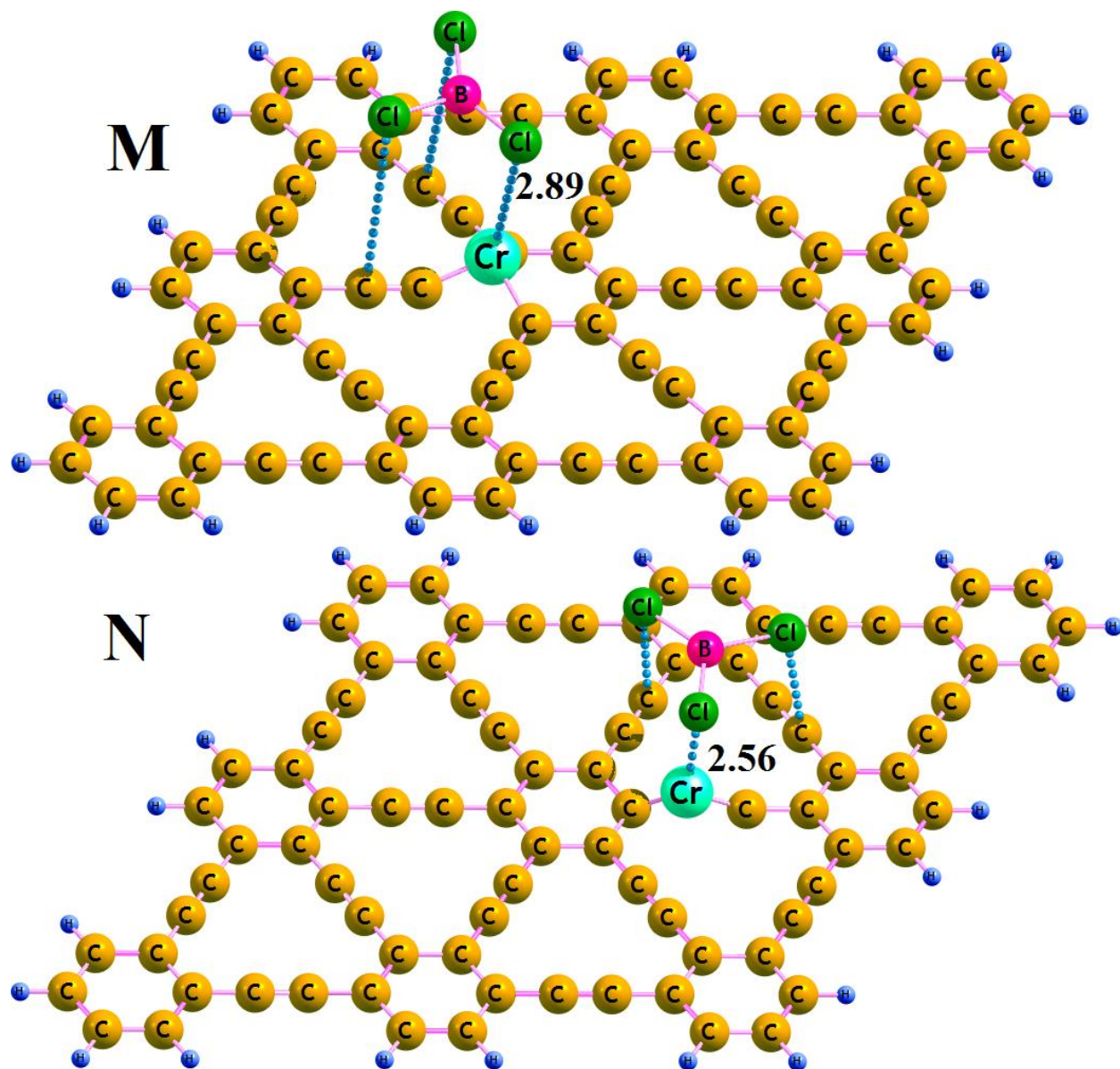


Fig. 7.

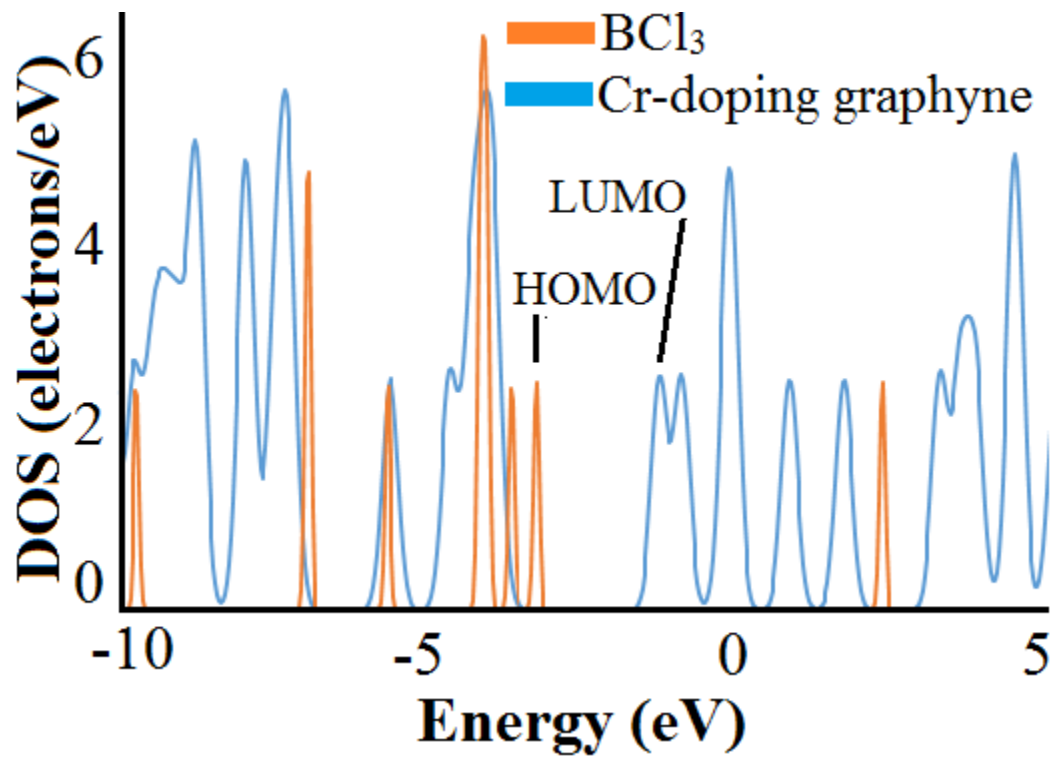
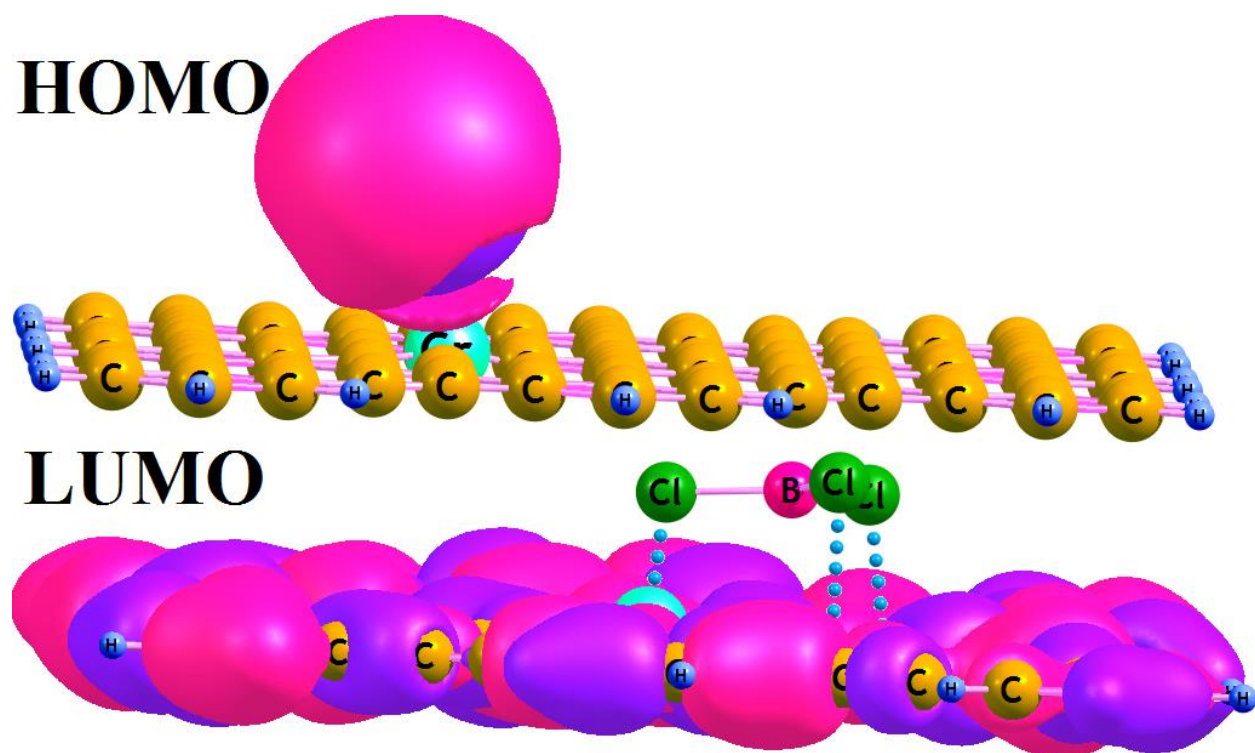


Fig. 8.



# Figures

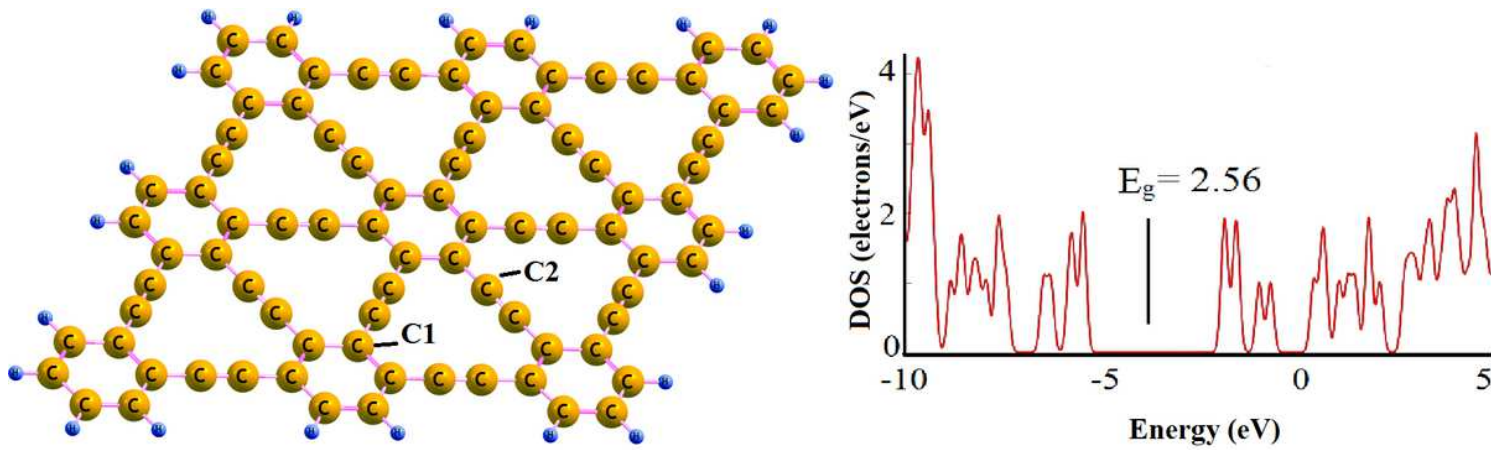


Figure 1

Optimized structure of graphyne and its density of state (DOS).

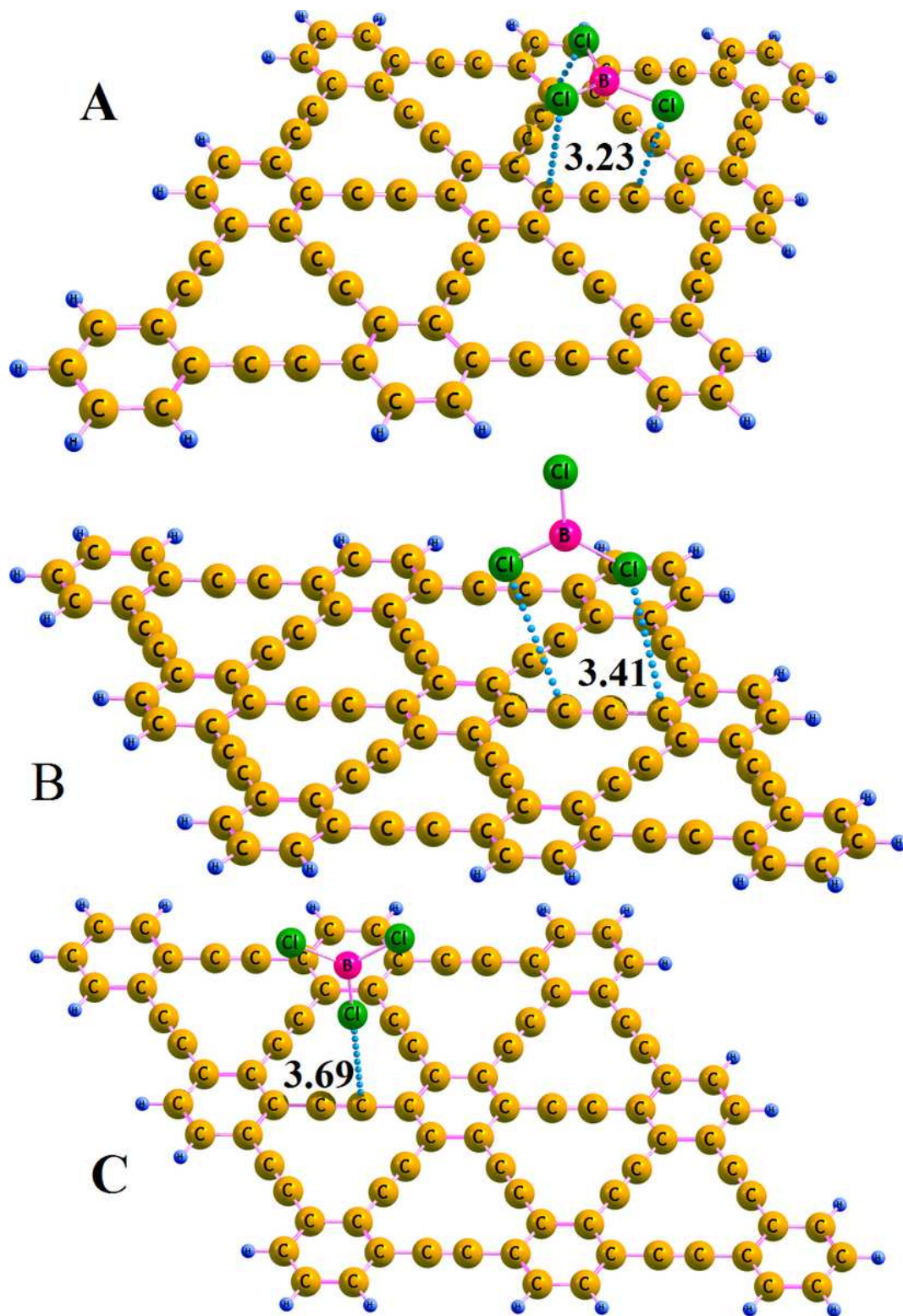


Figure 2

Models for three stable adsorption states for a BCl<sub>3</sub> molecule on the pristine graphyne, distances are in Å.

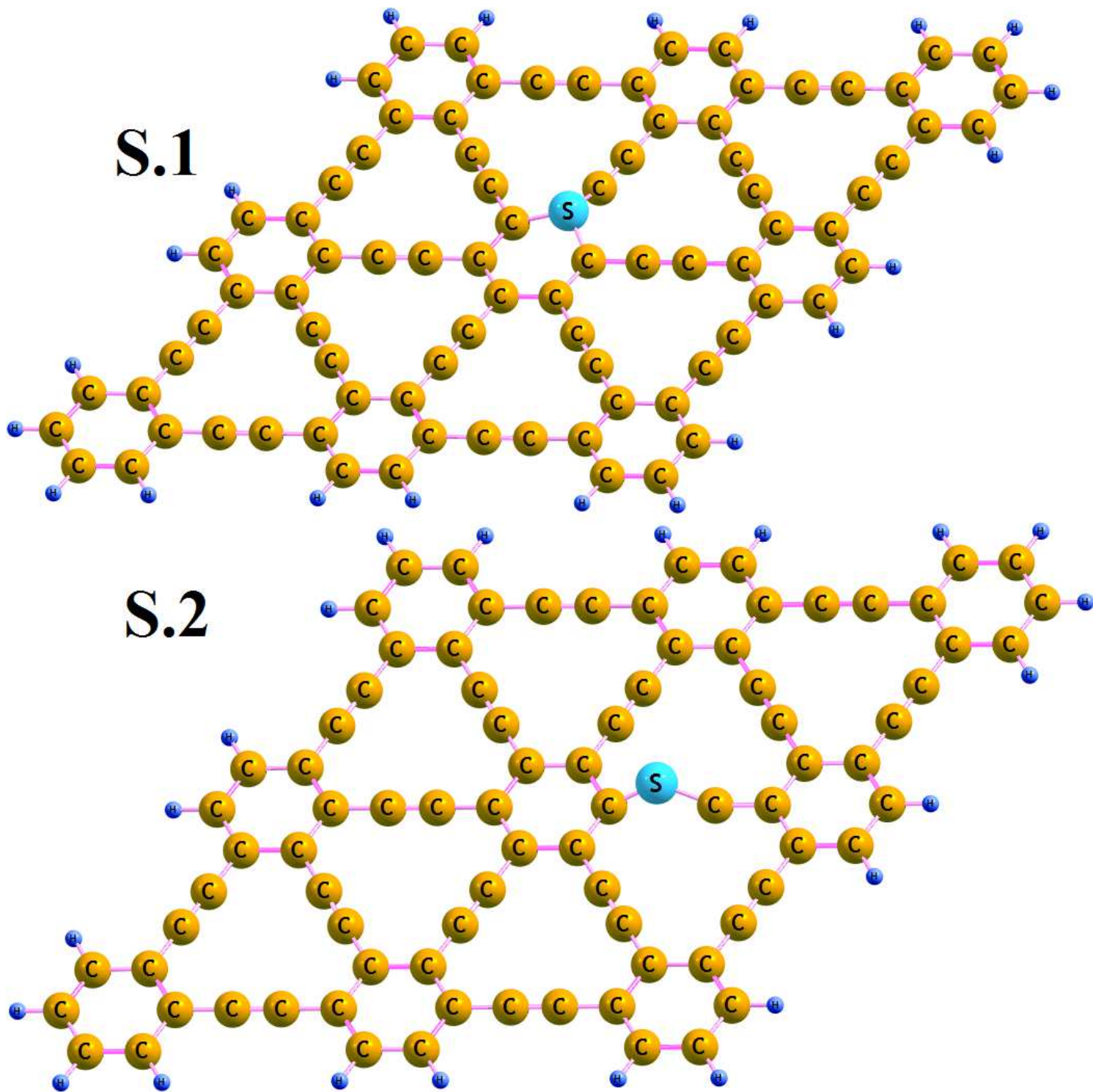


Figure 3

Optimized structures of different S-doped graphyne.

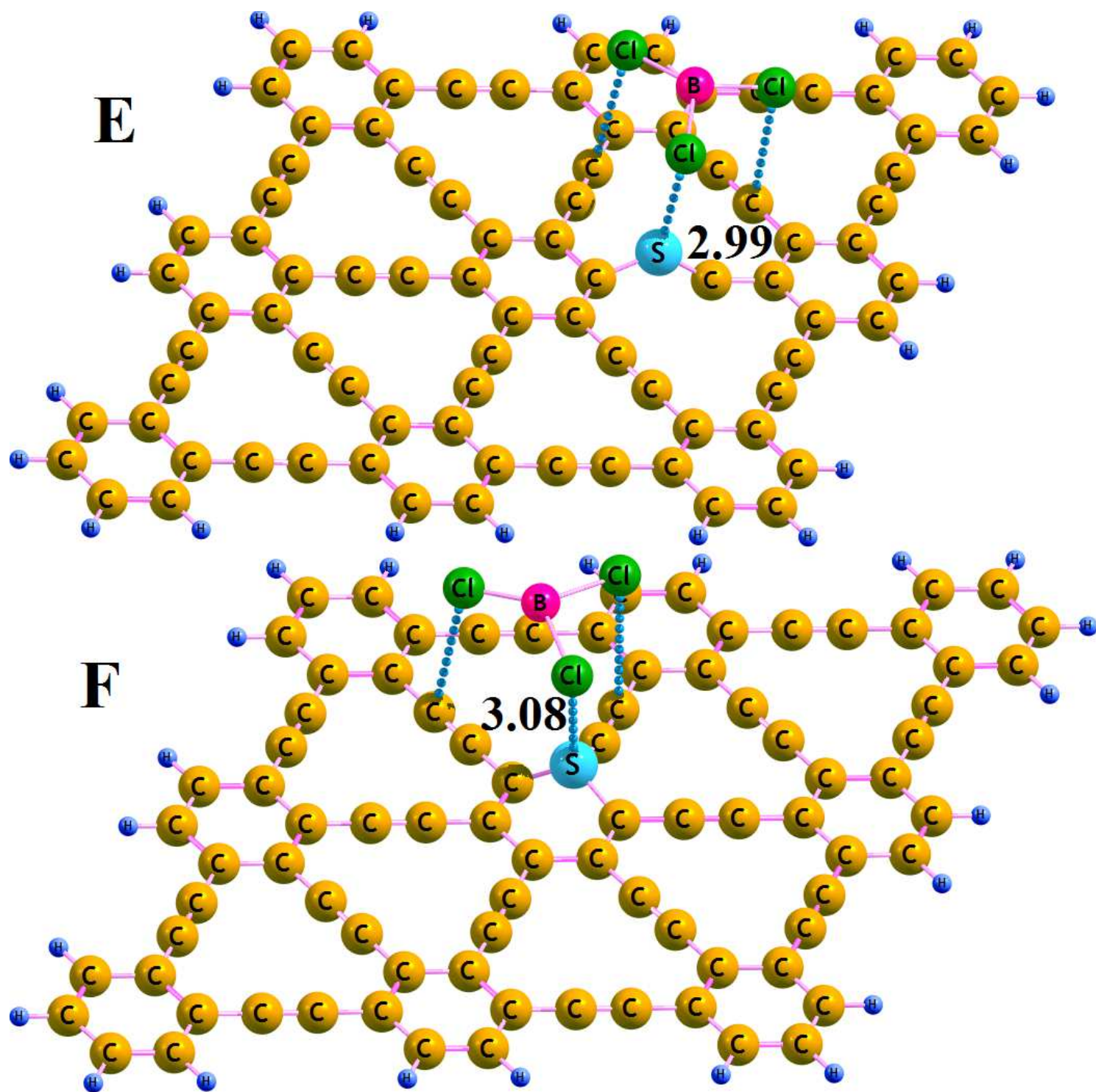


Figure 4

Models for two stable adsorption states for a BCl<sub>3</sub> molecule on the different S-doped graphyne, distances are in Å.

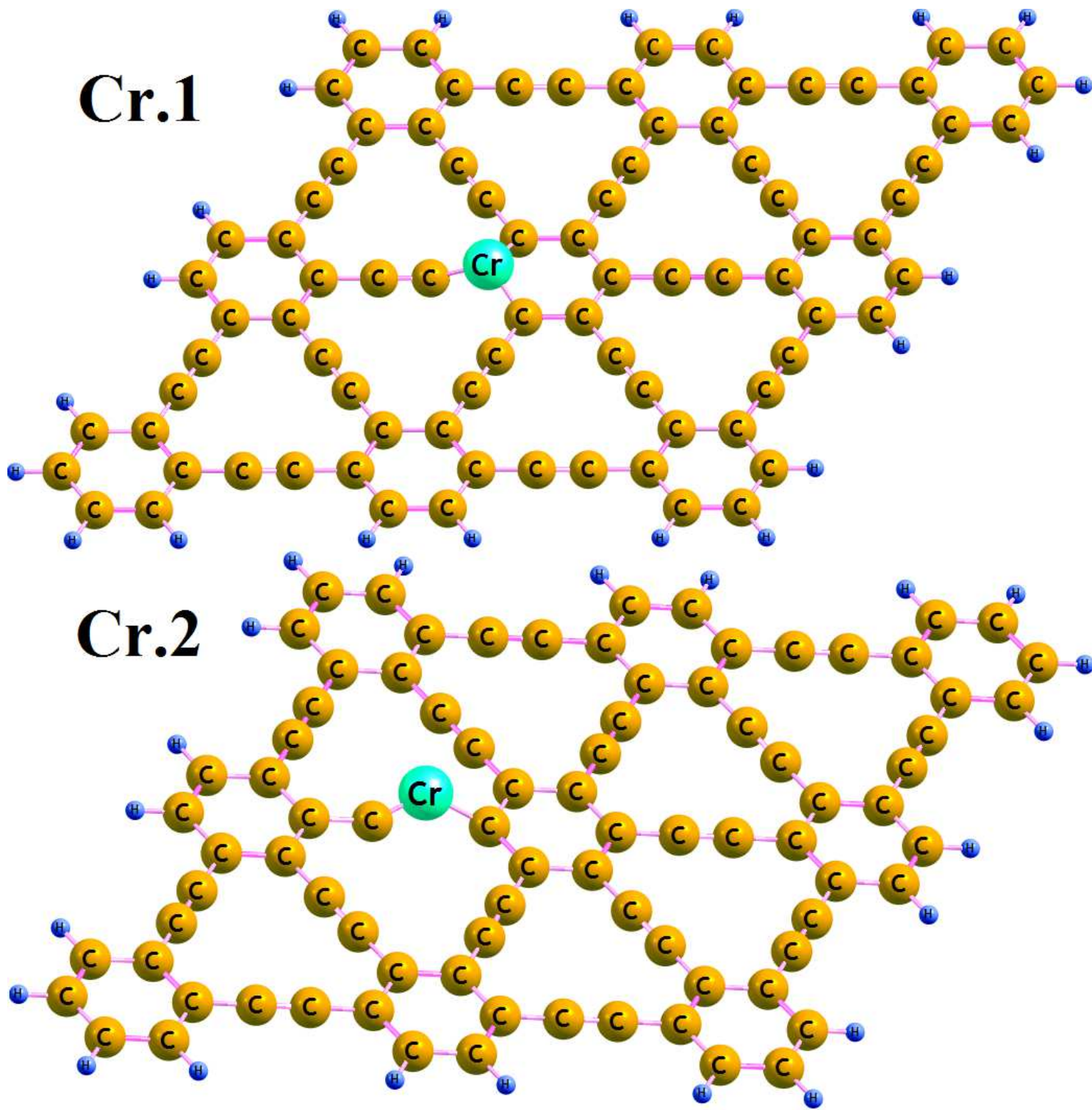


Figure 5  
Optimized structures of different Cr-doped graphyne.

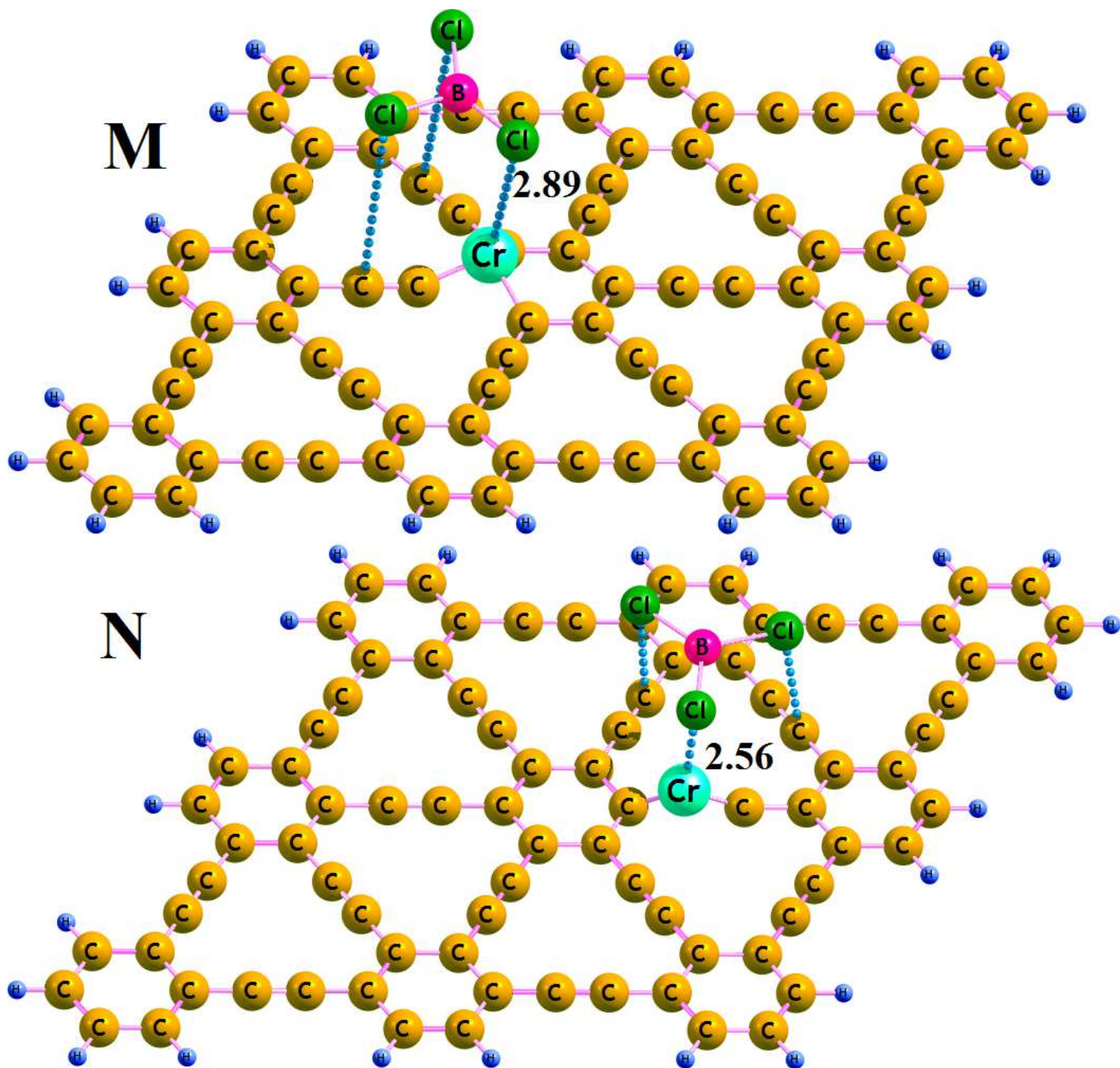


Figure 6

Models for two stable adsorption states for a BCl<sub>3</sub> molecule on the different Cr-doped graphyne, distances are in Å.

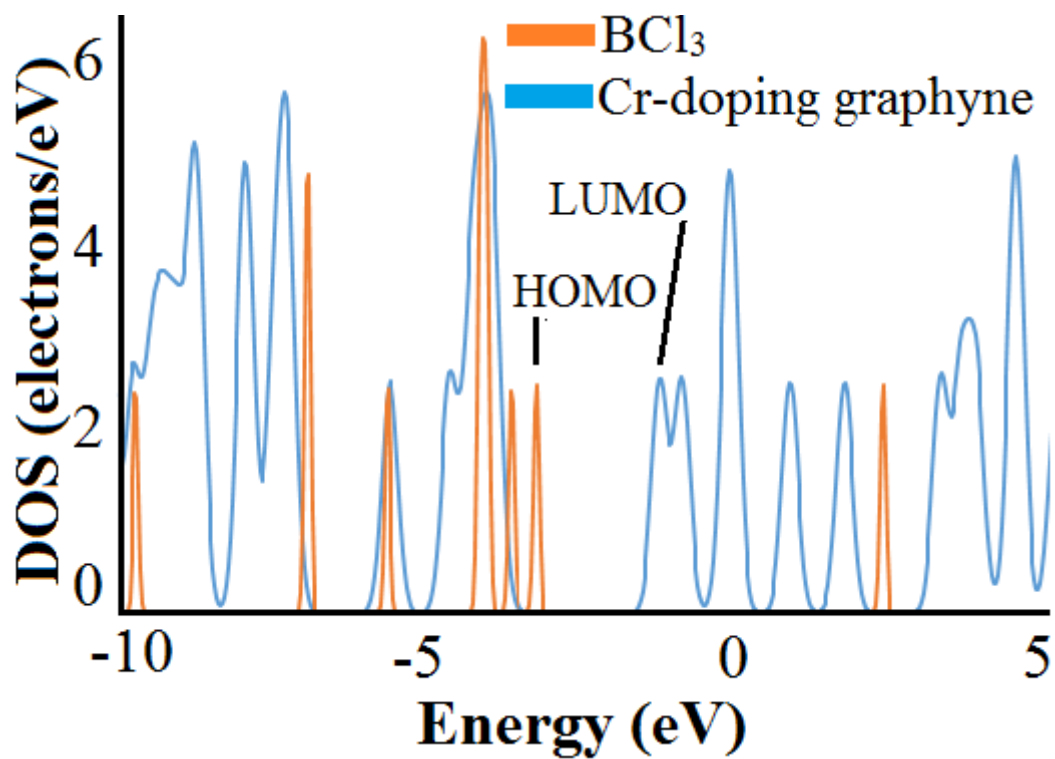


Figure 7

Partial DOS plot of Cr-doped graphyne/  $\text{BCl}_3$  nanostructure complex.

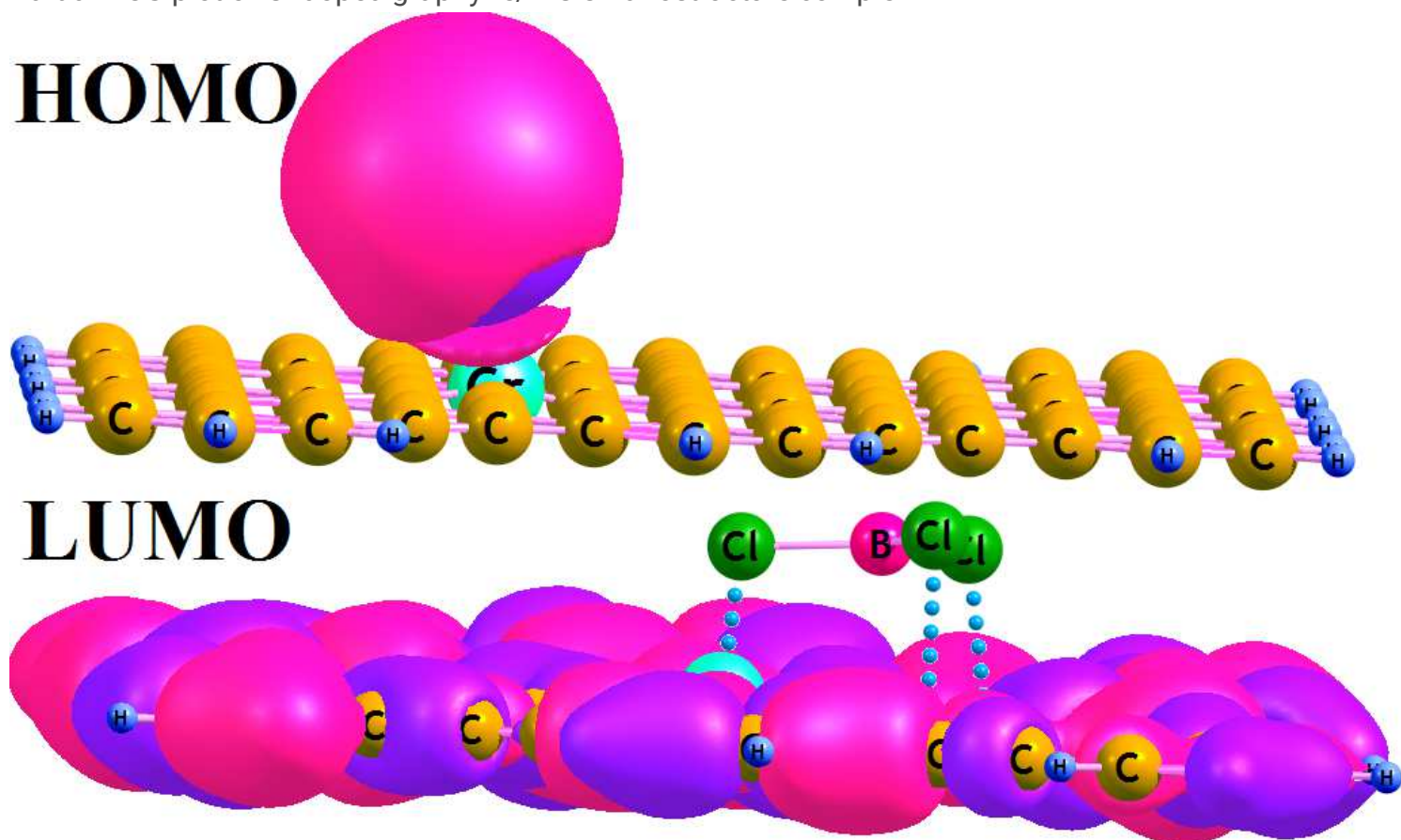


Figure 8

The HOMO profile of Cr-doped graphyne/ BCl<sub>3</sub> nanostructure complex.